Episodic outflows from SANE discs

Miljenko Čemeljić

Nicolaus Copernicus Astronomical Center, PAN
Warsaw, Poland
&
ASIAA Visiting Scholar, Taipei, Taiwan

This work was done during a Jan-Aug 2020 as a
SHAO Visiting Scientist (PIFI), CAS, Shanghai, China
in collaboration with
Prof. Feng Yuan & PhD student Hai Yang

Outline

- Introduction
- Full 3D GRMHD numerical simulation setup.
- Results in SANE simulations
- Formation of magnetic islands/flux ropes and reconnection layers
- Periodicity of the ejections.
- Summary

Introduction-episodic jets

•In the accreting systems, large scale jets are usually steady, while episodic jets are sometimes related to flares, which are observed on the smaller scale. One example is Sgr A*, the massive BH in the Galactic centre, where we observe radio, infrared and X-ray flares several times a day. Conclusion was that delays in peaks in the light curves at different wavebands and their fast rise and slow decay in the brightness and polarisation are related to the ejection and expansion of plasmoids from the accretion flow.

•Knots in the jets are also observed, e.g. in 3C 120 and M87, and could be related to episodic emission.

•There are models, like e.g. Blandford & Znajek (1977) and Blandford & Payne (1982) for continuous jets, but we still do not have a viable model for episodic jets.

•In Yuan et al. (2009), a model was proposed in analogy with Coronal Mass Ejections (CMEs) in the Sun. The closed magnetic field lines are emerging from the main body of the accretion flow and are expelled to the corona region. The footpoints of the magnetic loops are positioned in the turbulent accretion flow, and their twisting results in magnetic reconnection, forming the flux ropes. Because of the ongoing reconnection below such a flux rope, the magnetic tension force weakens, and the initial equilibrium between the magnetic tension and the magnetic pressure is not maintained, the flux ropes will be accelerated outwards, forming the episodic jet. The flares, observed from such jets, are from the emission originating from the electrons accelerated by the reconnection.

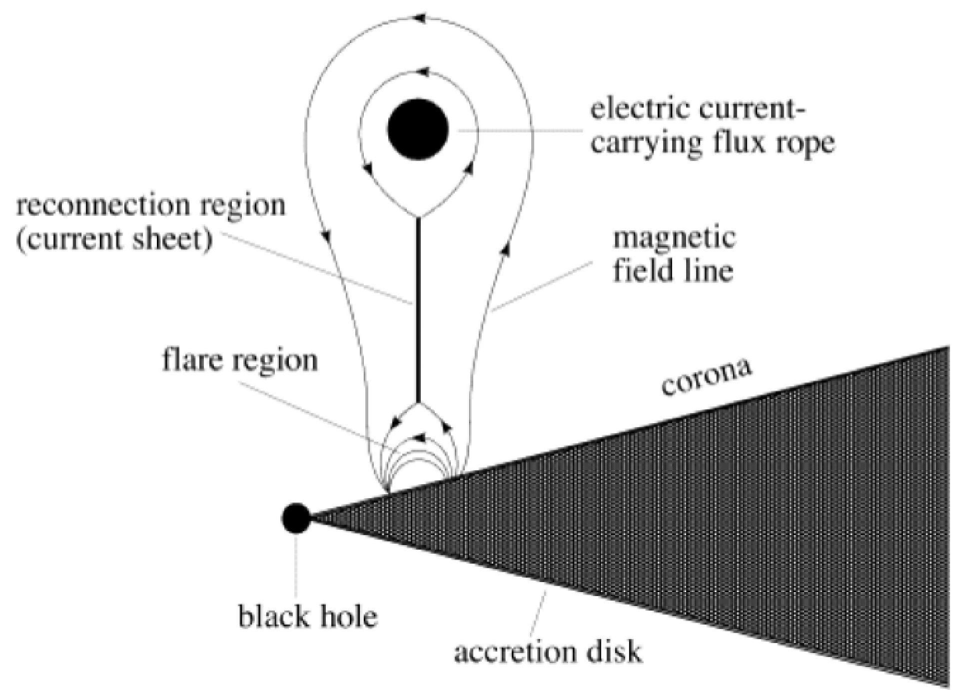

Fig. 1b from Yuan et al. (2009).

•In Shende et al. (2019) another model, in analogy with Toroidal Instability from tokamak research, was proposed-also used to model the CMEs.

Introduction-MAD and SANE simulations in 2D

•Nathanail et al. (2020) presented results of 2D ideal GRMHD simulations with the Black Hole Accretion Code (BHAC, Porth et al. 2017), with Adaptive Mesh Refinement (AMR) of both Magnetically Arrested and Standard and Normal Evolution (MAD and SANE) discs, with the different initial magnetic field configurations, in resolutions Rxϑ equal to 2048x1024, 4096x2048 and, for Model D, 6144x3072 grid cells (resolution is important because of numerical dissipation). They obtain results with formation of copious plasmoids and describe formation and movement of plasmoids.

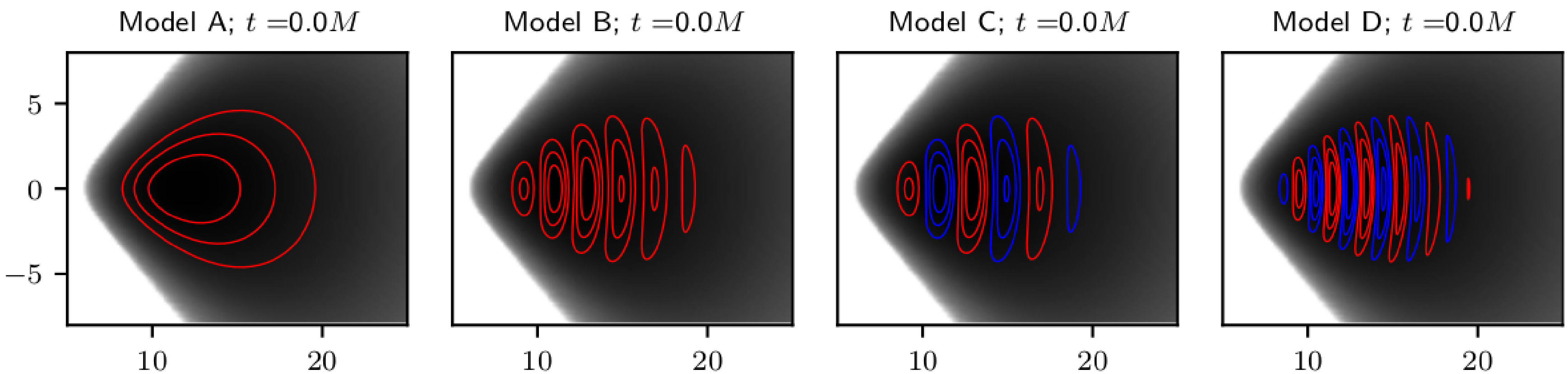

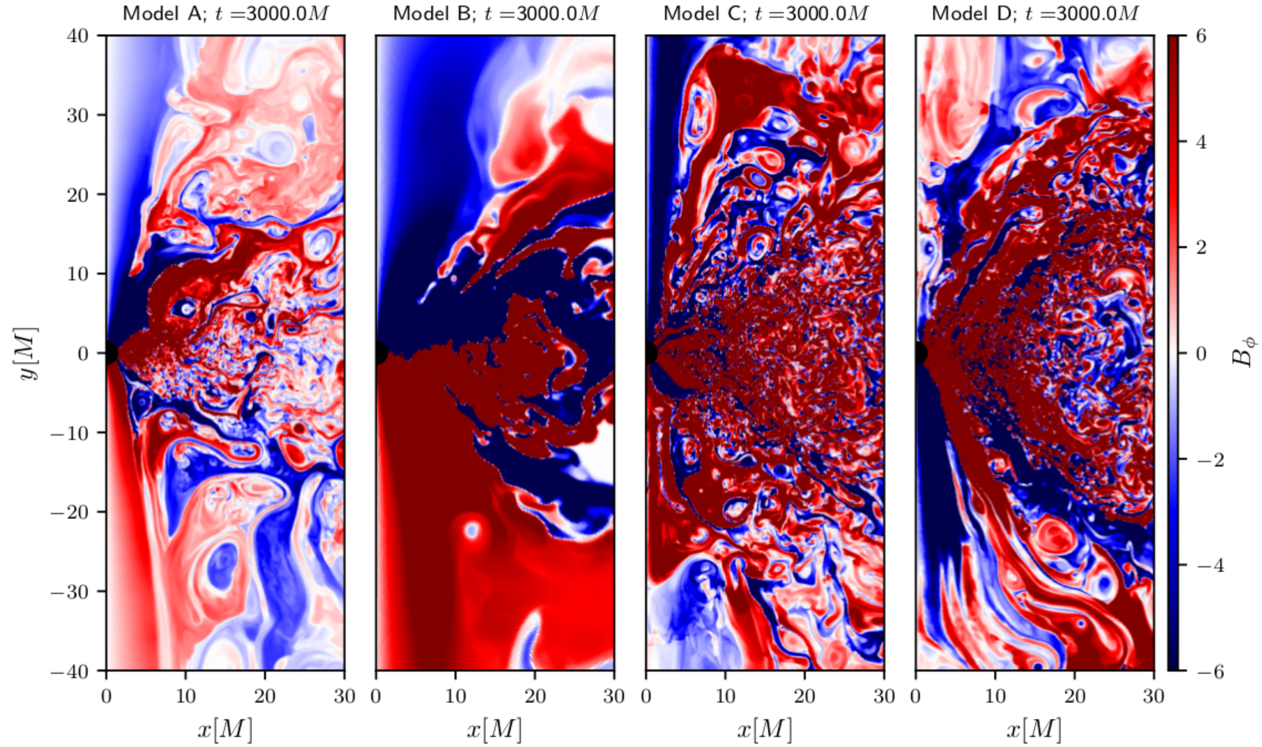

Figure 6. The B_ϕ component of the magnetic field for the four models at time $t = 3000\ M$. The red and blue regions denote regions where the magnetic field has different polarity. The resolutions are: base resolution for `Model B`, 4× base resolution for `Models A`, `C` and `D`.

Introduction-MAD and SANE simulations in 2D

•Plasmoids move outwards, in 3D rendering they would spiral out of the system (Nathanail et al. 2020):

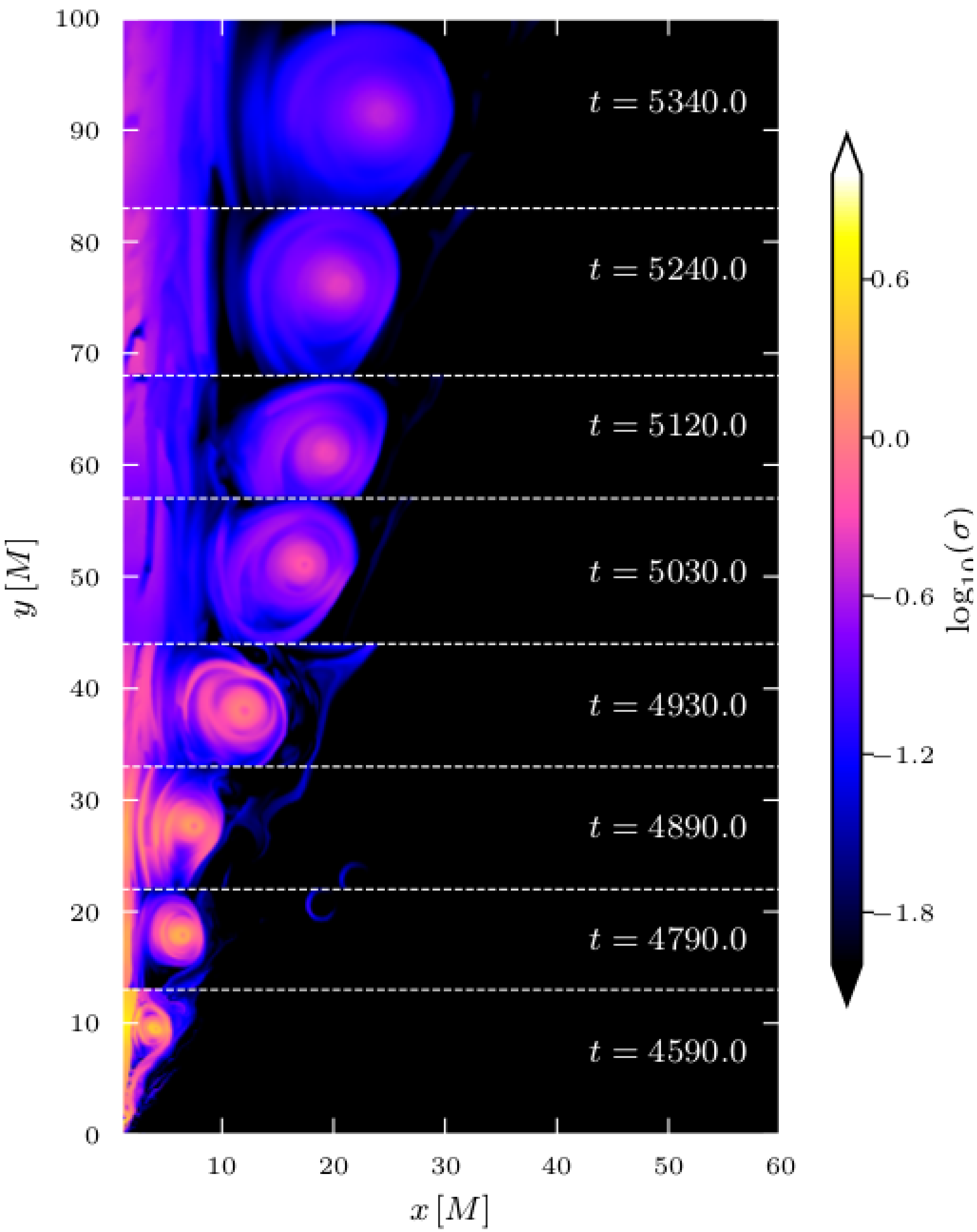

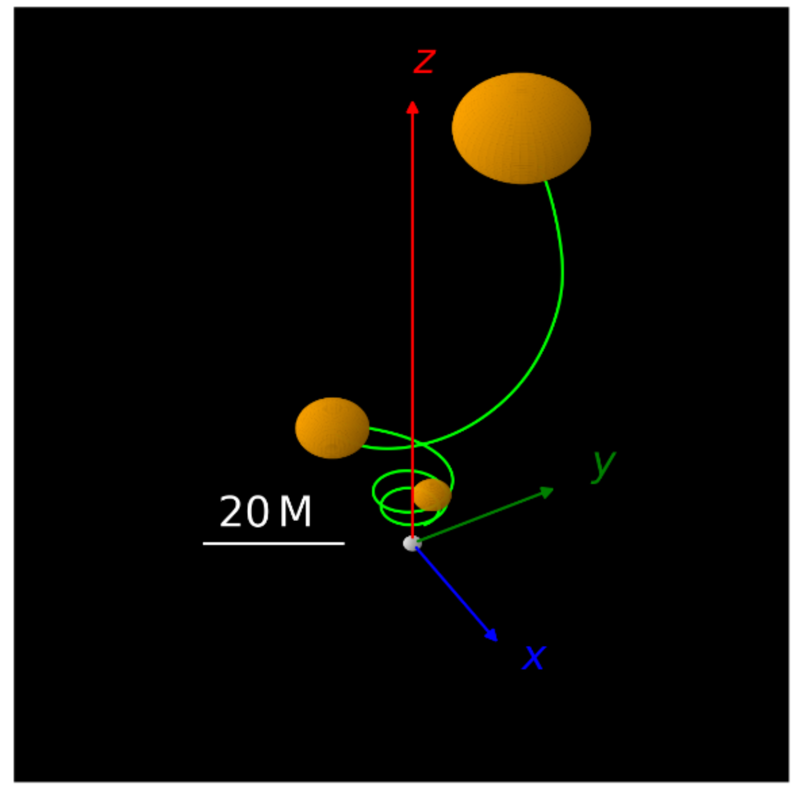

Figure 10. 3D reconstruction of the trajectory of the outward moving plasmoid shown in Fig. 9 after integrating in time the velocity of its core, including the azimuthal component.

Measuring of the plasmoids

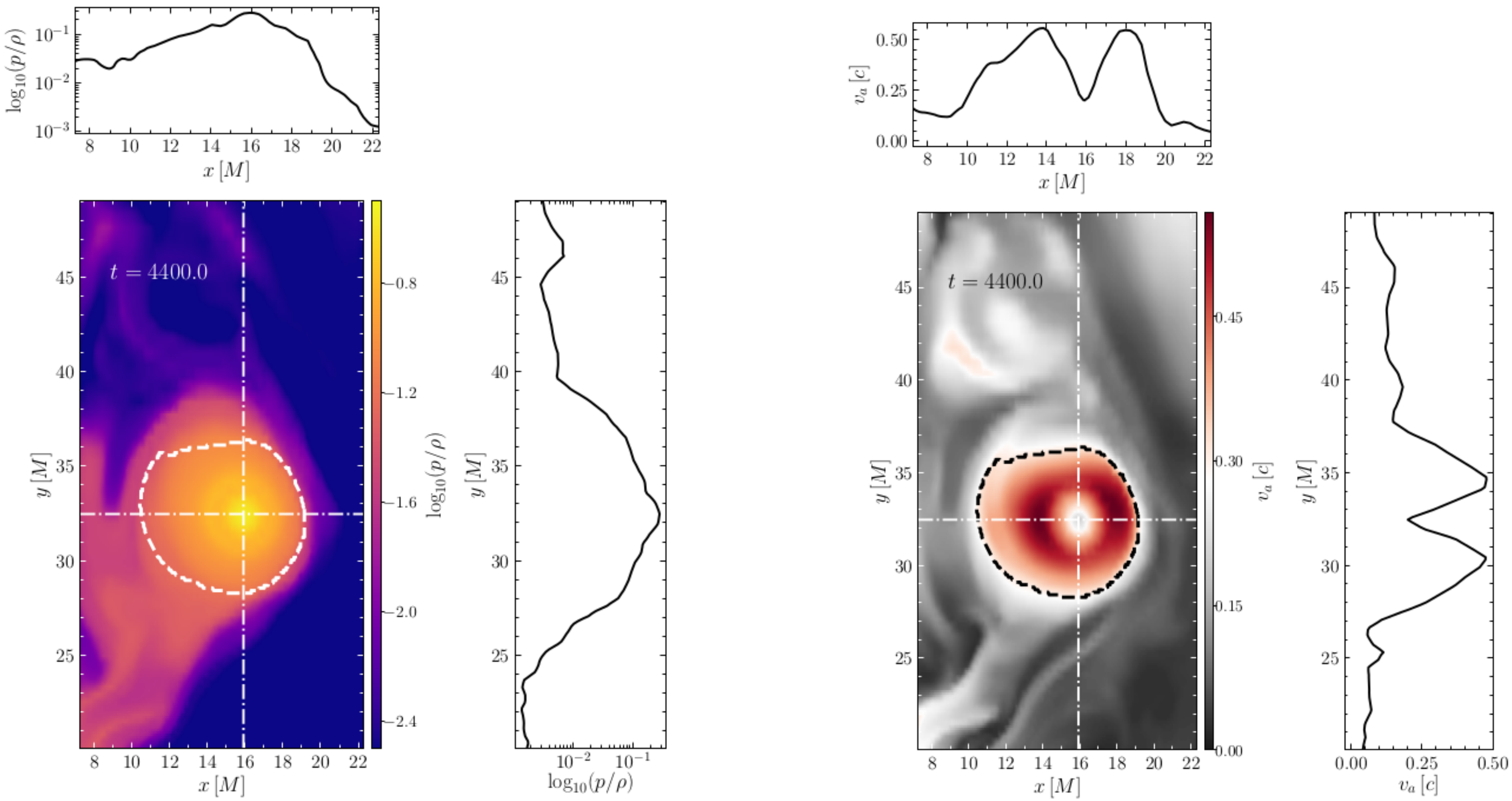

Figure 12. Detection of a plasmoid from `Model D` for either the temperature proxy (left panels) or the Alfvèn speed (right panels). The two (horizontal and vertical) dashed lines pass though the center of the plasmoid. The two subplots show exactly the cuts made by these lines through the plasmoid.

Introduction-MAD and SANE simulations in 2D

In Ripperda et al. (2020) presented are similar, but resistive 2D GRMHD simulations with the same code, BHAC. In their simulations there is no difference in results between the ideal and weakly resistive simulations-with enough resolution reaching up to 6144x3072 grid cells, and showing that in half of this resolution results converge all the same. **Conclusion** is that ideal MHD results, with only the numerical resistivity dissipating the magnetic field, are capturing the physics in such simulations.

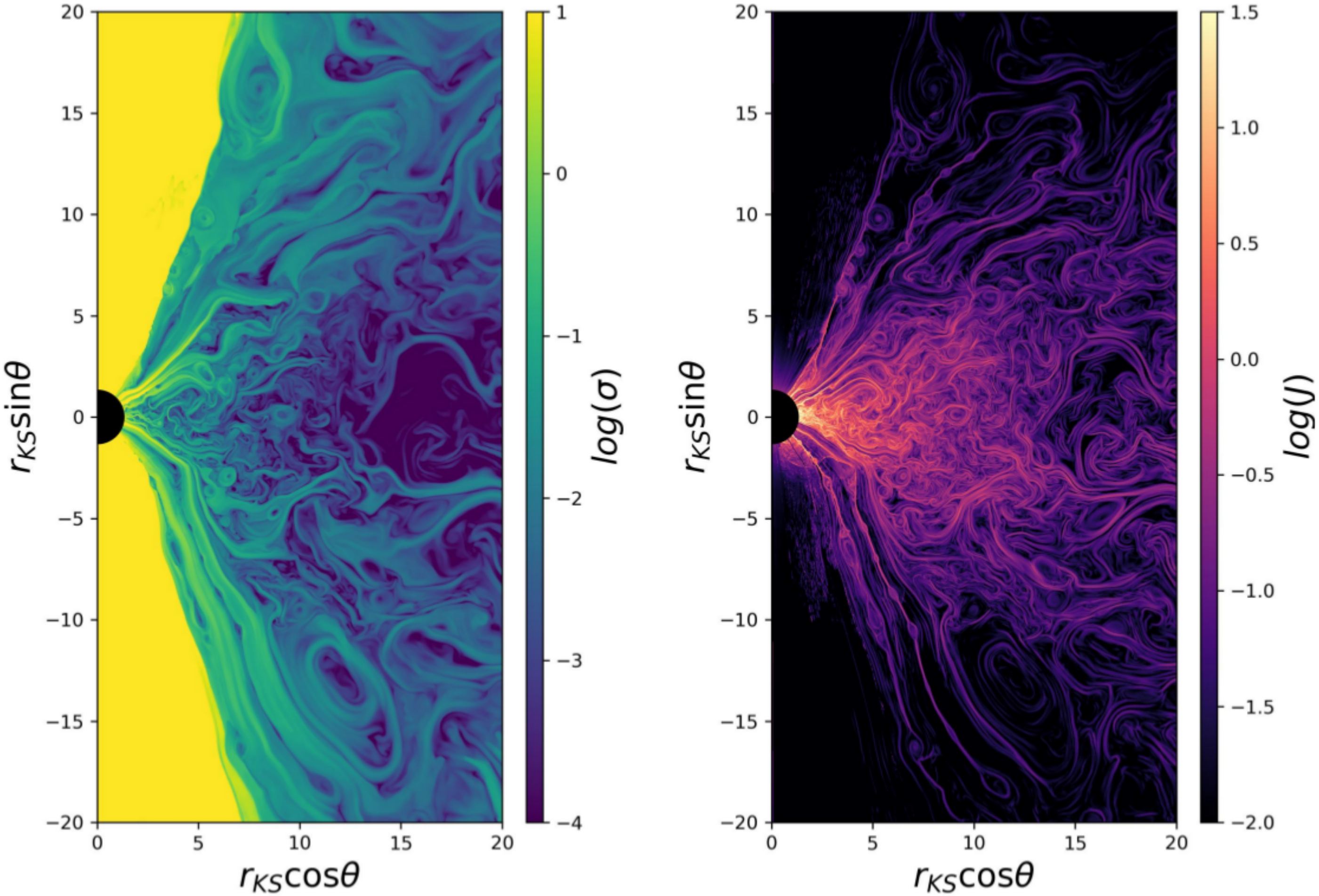

Snapshot in quasi-steady-state phase of accretion at t = 1540 r_g/c in SANE case. Magnetization $\sigma=B^2/\rho$ shows that current sheets along the jet's sheath are in the relativistic regime $\sigma >> 1$, whereas in the disk they are in the trans-relativistic regime $\sigma \leq 1$. The thin tearing-unstable reconnection layers are indicated by a strong current density in the right panel.

Results for SANE

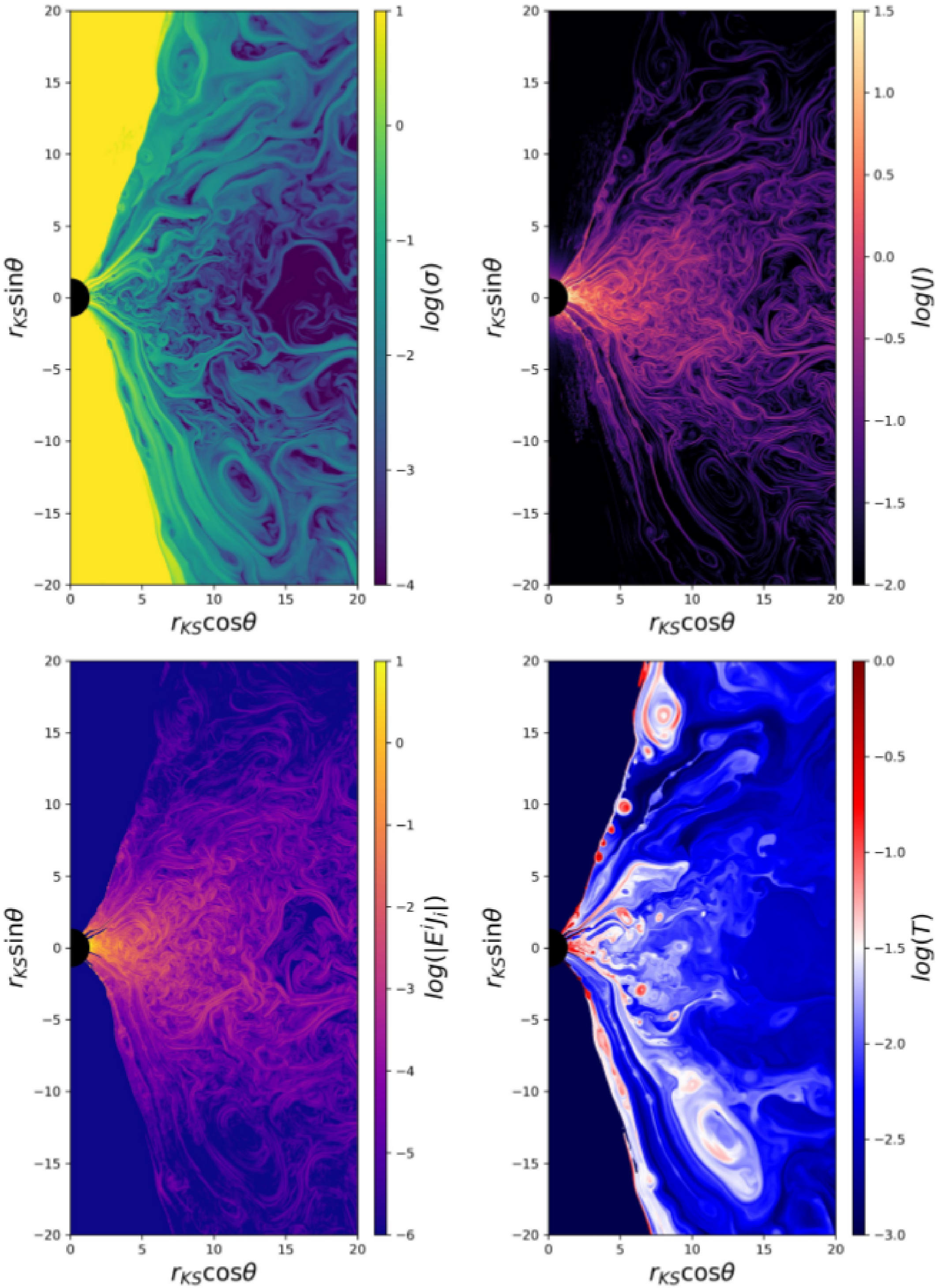

SANE quasi-steady-state phase of accretion at t = 1540rg /c. Top left: Magnetization σ showing that current sheets along the jet's sheath are in the relativistic regime σ >> 1, whereas in the disk they are in the transrelativistic regime σ ≲ 1. Top right: The thin tearing-unstable reconnection layers are indicated by a strong current density. Bottom left: Plasmoids in the current sheets are heated by Ohmic heating close to the event horizon. The strong parallel electric field indicated by E^iJ_i can accelerate particles to non-thermal energies. Bottom right: Plasmoids both in the disk and along the jet's sheath are heated up to relativistic temperatures T = p/ρ ∼ 1.

Results for MAD

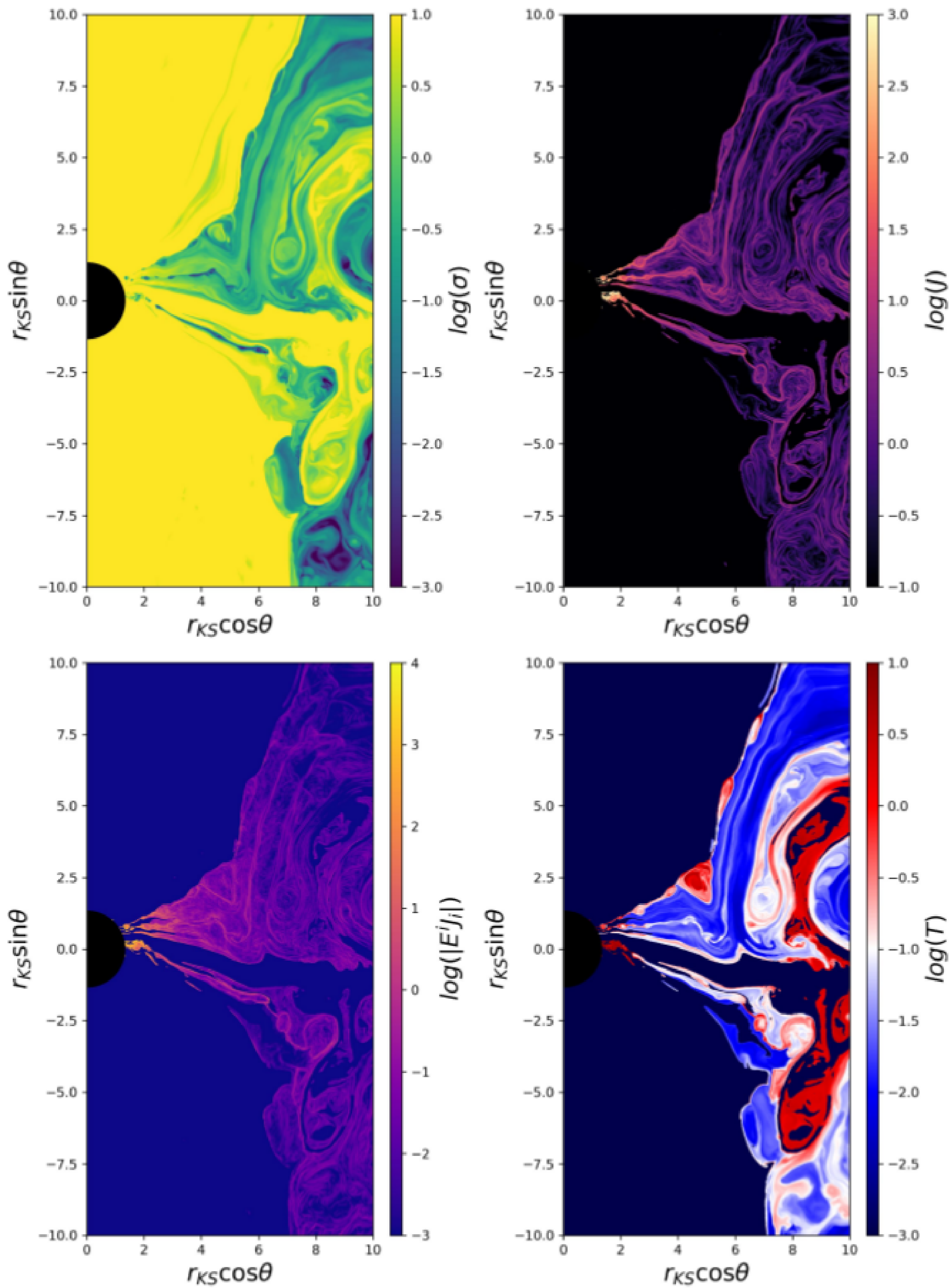

MAD, quasi-steady-state at t = 2971rg/c. Top left: Magnetization σ showing that current sheets close to the event horizon are in the relativistic regime σ>>. Top right: The thin tearing-unstable reconnection layers are indicated by a strong current density. Bottom left: Plasmoids in the current sheets are heated by Ohmic heating close to the event horizon. Bottom right: Plasmoids formed in the equatorial sheets are advected into both the disk and along the jet's sheath and are heated up to relativistic temperatures T = p/ρ ∼ 10, an order of magnitude larger than in the SANE case.

Our numerical simulations setup

•In the BH Accretion and High Energy Astrophysics group in SHAO, numerical simulations were performed using the GRMHD code Athena++ (White et al. 2016) in full 3D, solving the ideal MHD equations in the Kerr metrics, in Kerr-Schild (horizon penetrating) coordinates (t, R, θ, φ).

•Resolution is Rxϑxφ=[288x128x64] grid cells in spherical coordinates, in a physical domain reaching to 2500 gravitational radii; with different refinements in the **static mesh refinement**,

to obtain largest resolution where it is most needed.

•Staggered mesh **Constrained Transport** method is applied to maintain the divergence-free magnetic field.

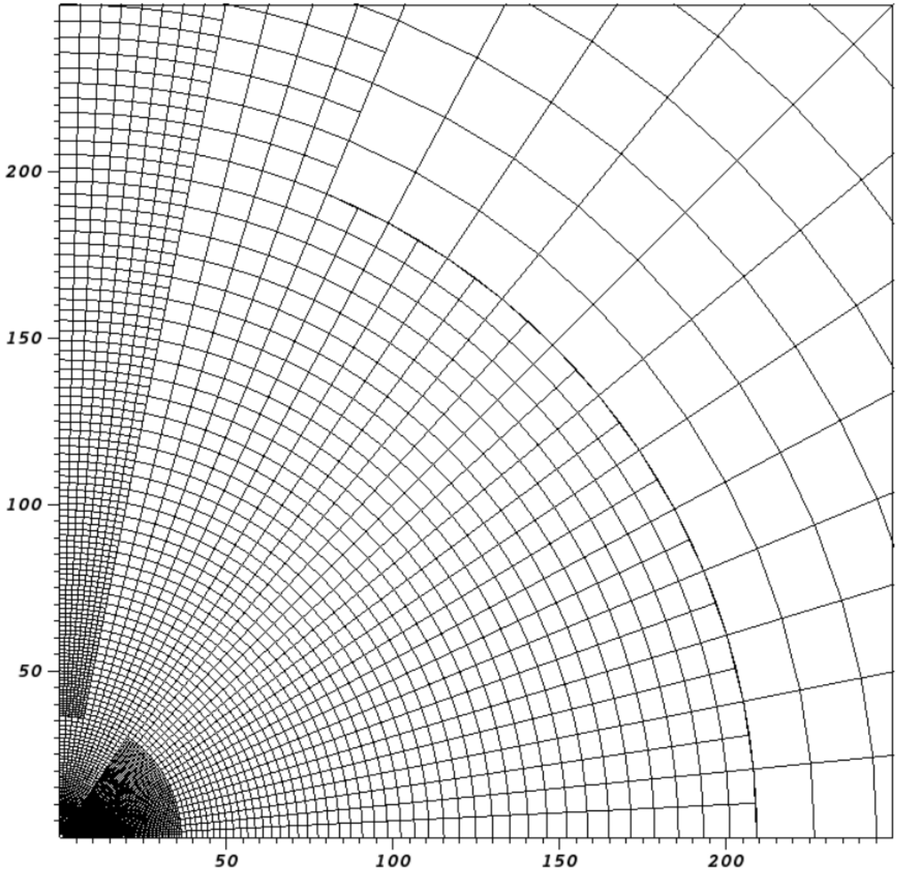

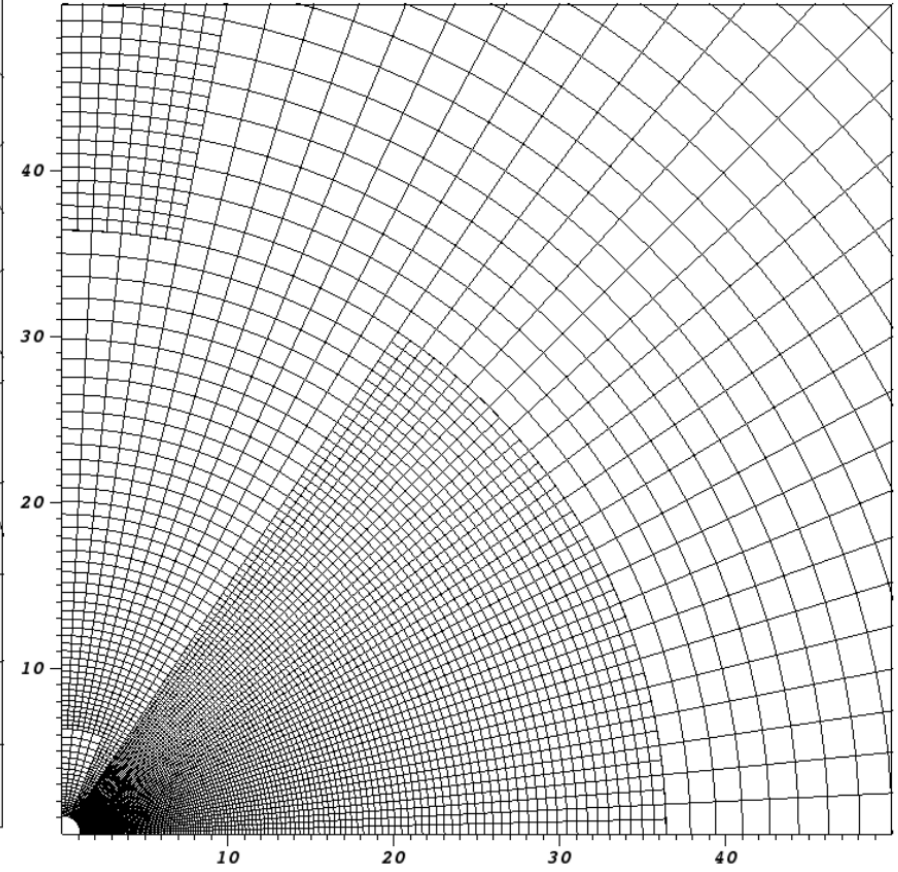

Initial conditions

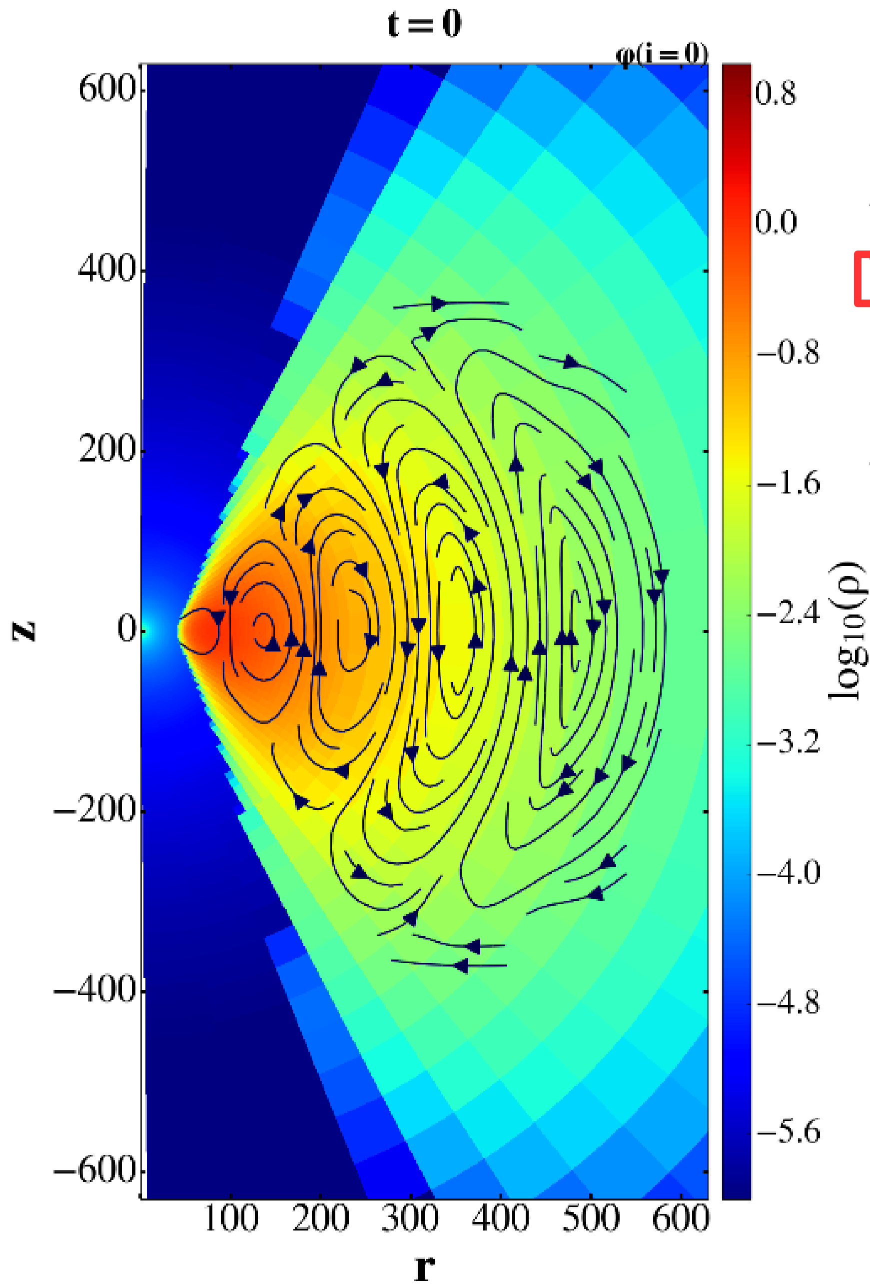

Fig. 1. Density in a logarithmic colour grading and a poloidal magnetic field contained inside the torus around a black hole in our SANE setup. Loops of poloidal magnetic field are shown with solid lines, with arrows showing the clockwise and counter-clockwise direction of the initial loops of magnetic field.

Table 1. Parameters used in different cases in our simulations.

Model	a	β_{min}	N_r	N_θ	N_ϕ	*Duration*
SANE00	0	0.05833	288	128	64	40000
MAD00	0	0.1	288	128	64	40000
SANE98	0.98	0.03	352	128	64	40000
MAD98	0.98	0.1	352	128	64	40000

Formation of the magnetic islands

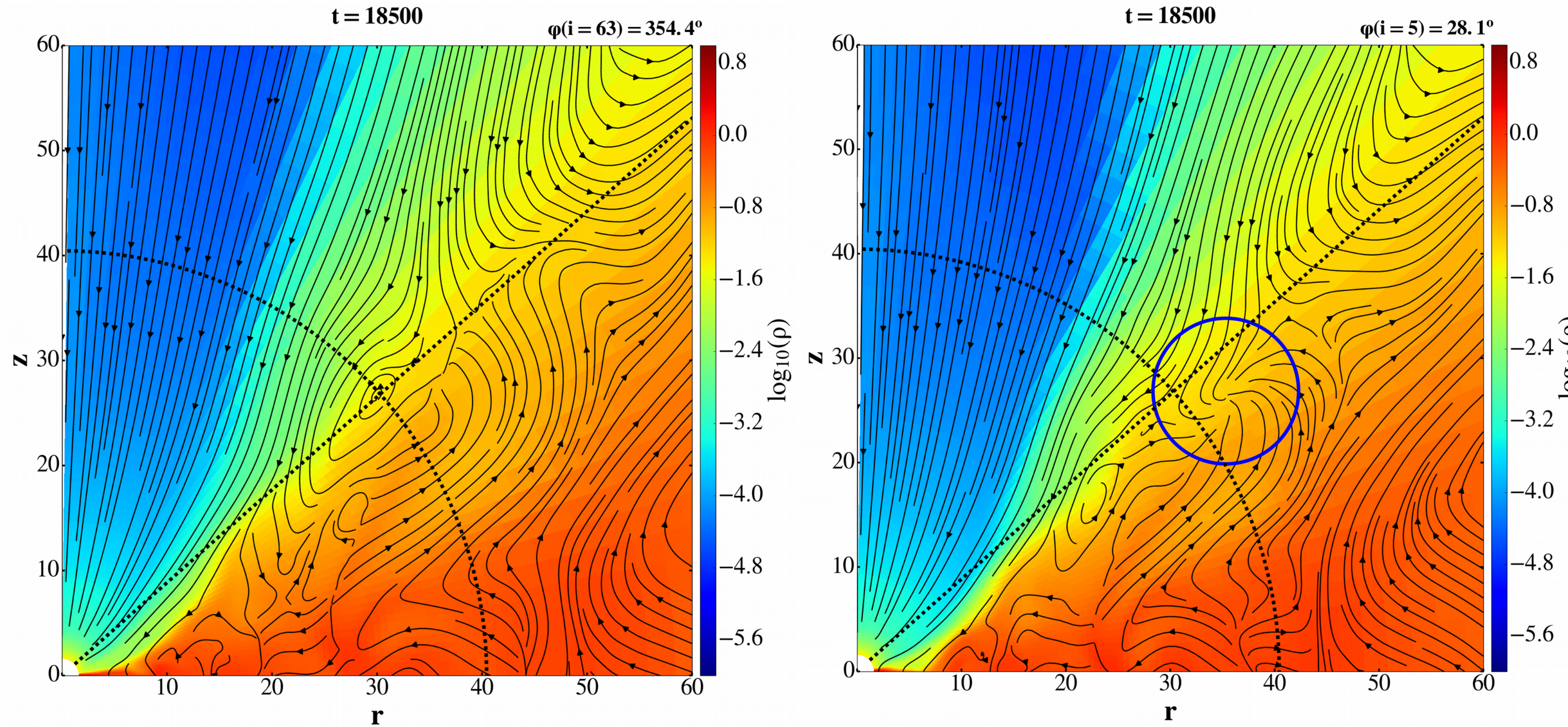

Left panel: Magnetic islands form along the disk-corona boundary. Solid lines are the poloidal magnetic field lines, with arrows showing the direction of magnetic field. *Right panel*:When an axis of the flux rope is not perpendicular to the (R, θ) plane at the chosen azimuthal angle φ, poloidal magnetic field lines will be seen as whirling around the center of the flux rope (encircled with a blue circle here), not as a circular magnetic island. Field lines are twisted near the footpoint of the flux rope.

Results in the SANE simulations in 3D

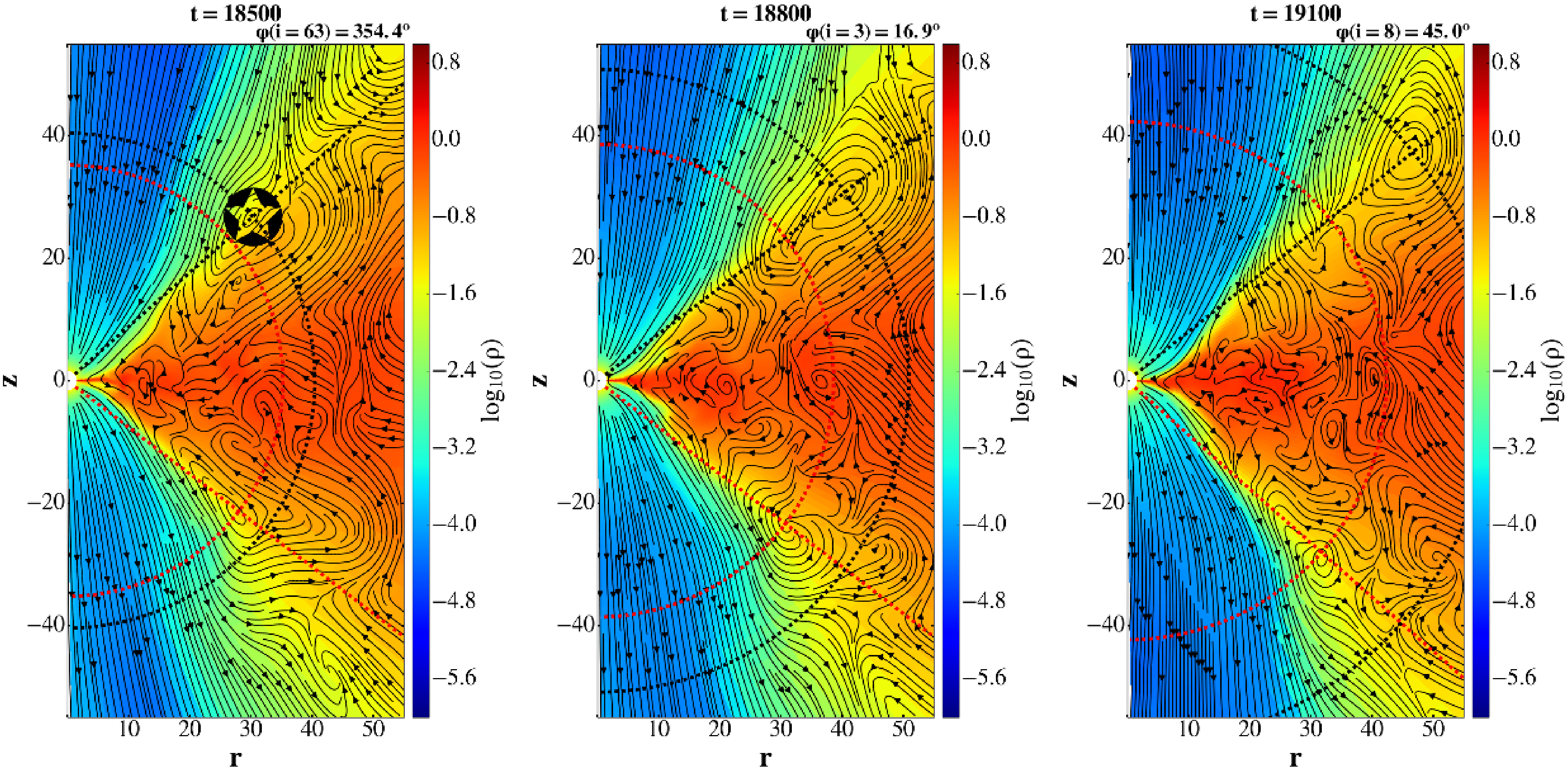

Snapshots at three different times in our simulation, showing density in logarithmic colour grading, overplotted with poloidal magnetic field lines, with arrows showing the direction of the poloidal magnetic field. We describe the motion of the magnetic islands by tracing the positions of their centres. A star mark in the left panel denotes the magnetic island above the equatorial plane.

Density and magnetic field components along the flux rope

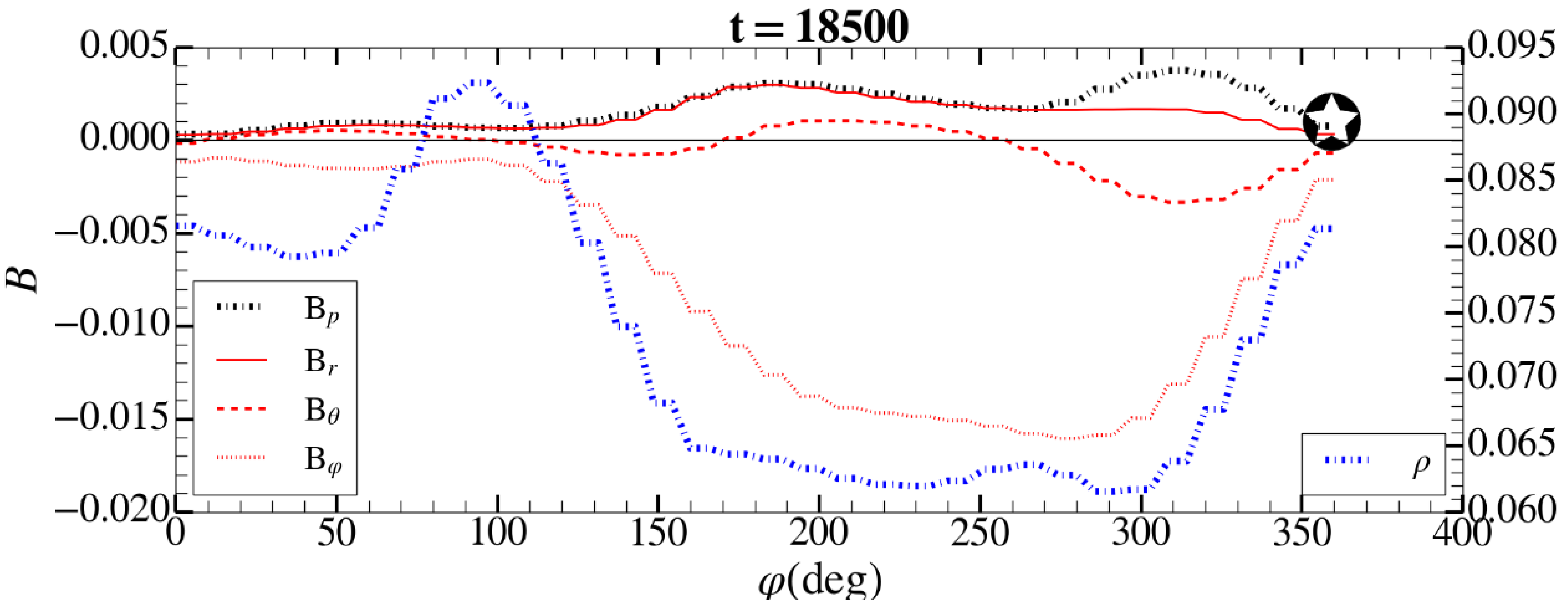

The φ-profiles of various components of magnetic field and density of the flux rope. Since the cylindrical radius of the flux rope at different φ is not a constant, in this figure the flux rope is present only at two places, i.e., φ ~ 100 deg and φ ~ 350 deg.

Magnetic flux rope in the φ-z plane

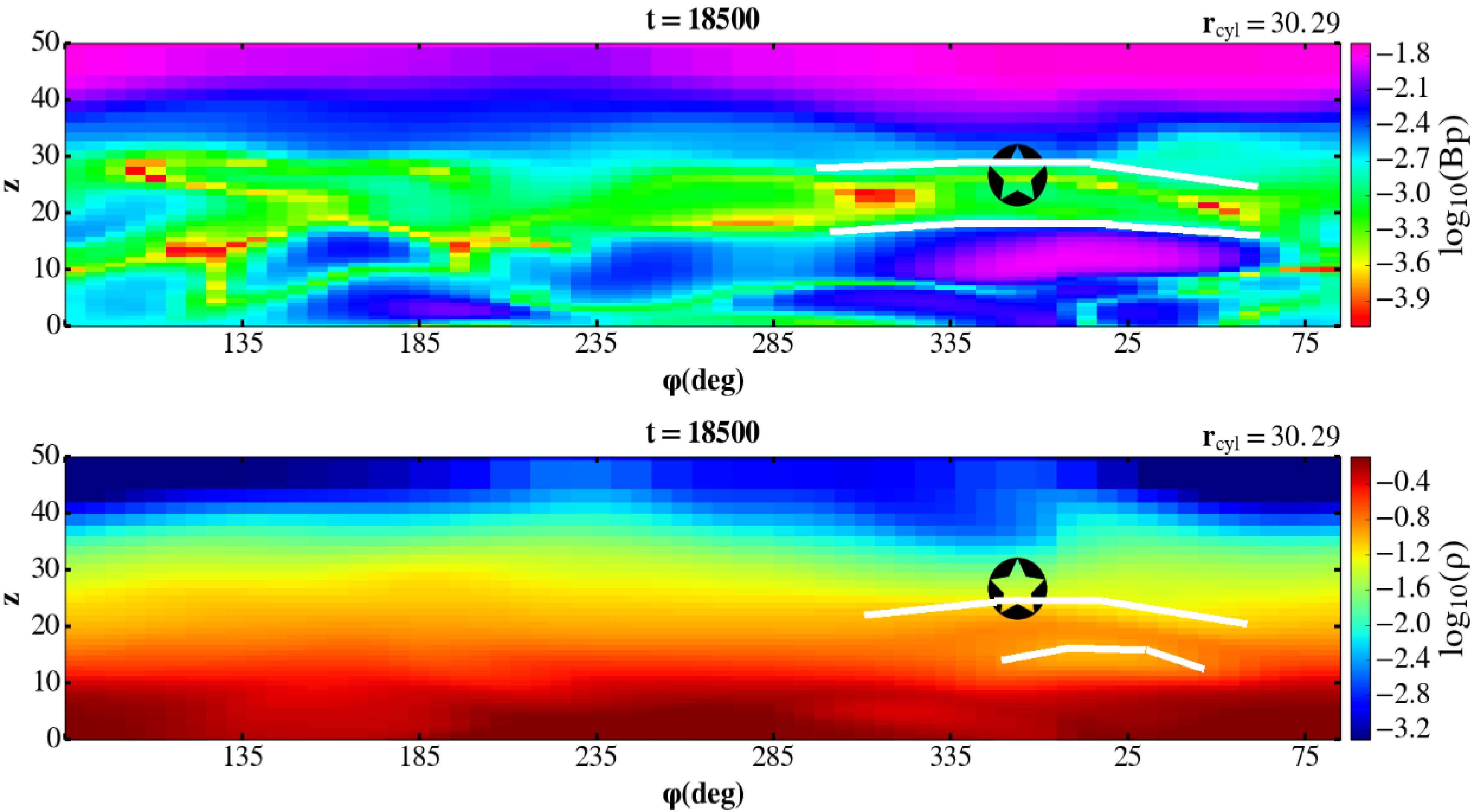

Top panel: Distribution of the poloidal magnetic field strength in the $\varphi - z$ plane with a constant cylindrical radius $r_{cyl} = 30.29$ above the equatorial plane at $T = 18500\ r_g/c$. The star mark denotes position of the magnetic island from previous figures. The poloidal field reaches a local minima at the center of the flux rope, which is shown as a slice through the azimuthal extensions of the magnetic islands (i.e., the green "belt" bounded by the white lines). Parts of the arcs of the flux ropes lie in this plane. *Bottom panel*: Distribution of density in the same $\varphi - z$ plane.

Where the islands form and how they move?

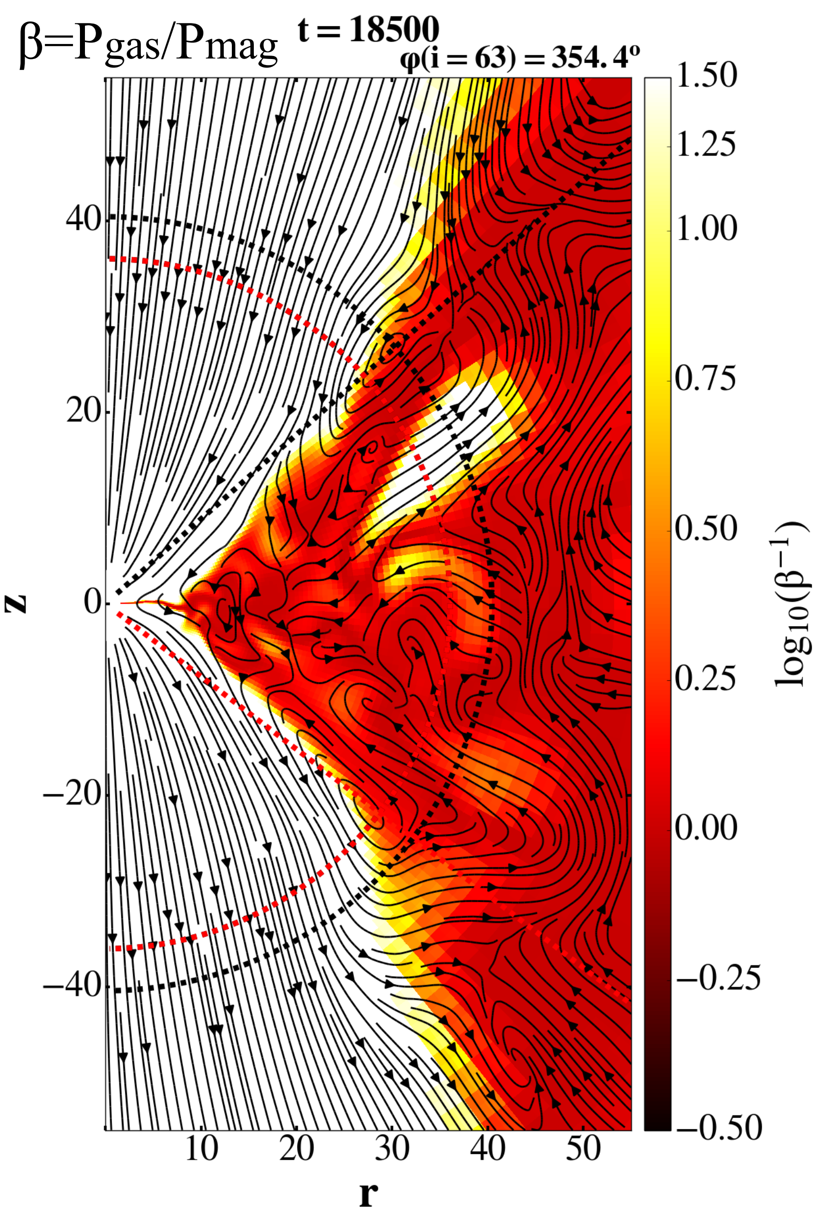

Magnetic islands form near the disk surface where plasma β∼1.

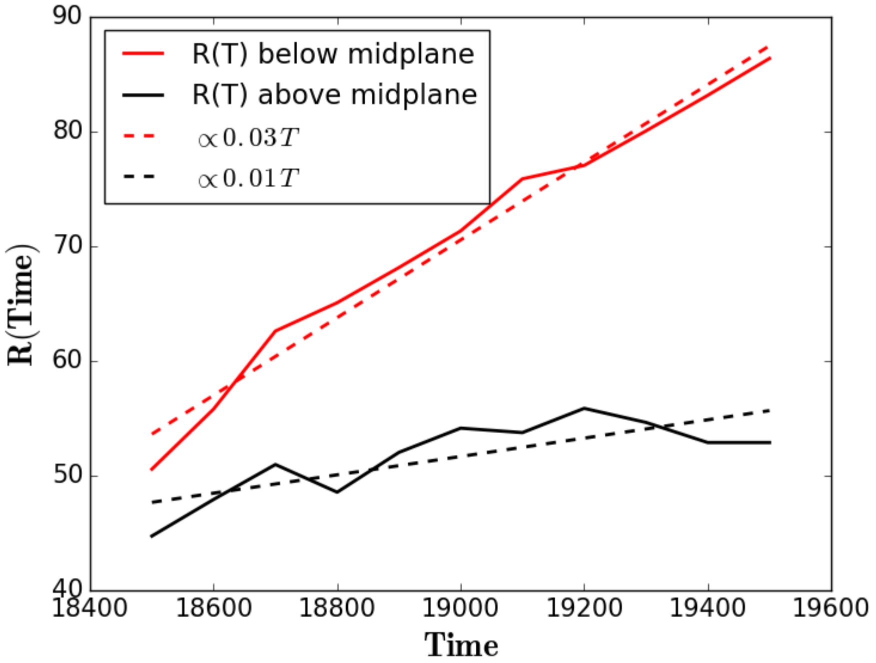

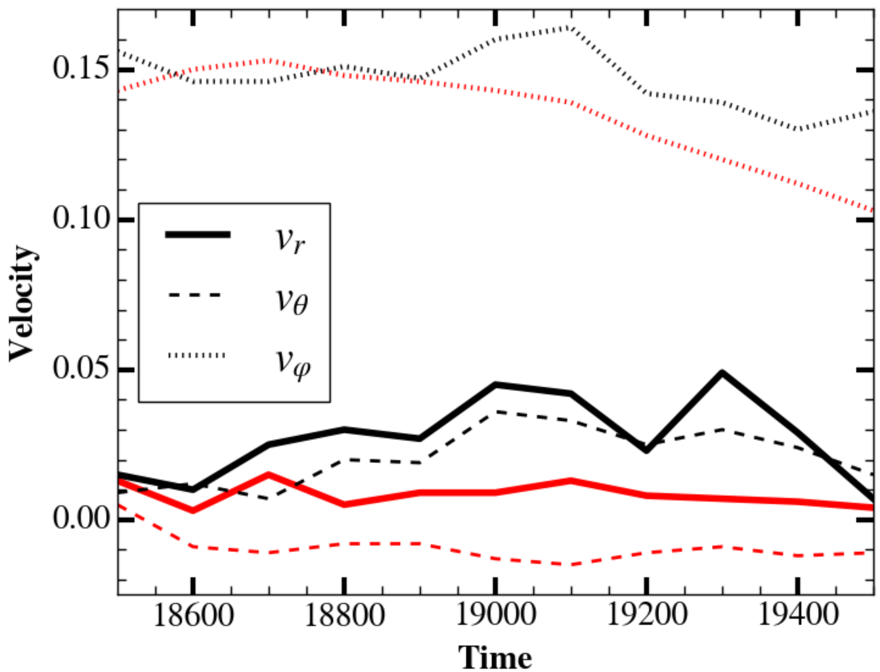

Top panel: Positions in time of the two mag. islands above (black) and below (red) the equatorial plane. Slopes of least square fits denote the radial velocity of the islands, 0.03c and 0.01c, respectively. Bottom panel: Time dependence in various components of the magnetic island velocity.

Forces on the magnetic flux rope

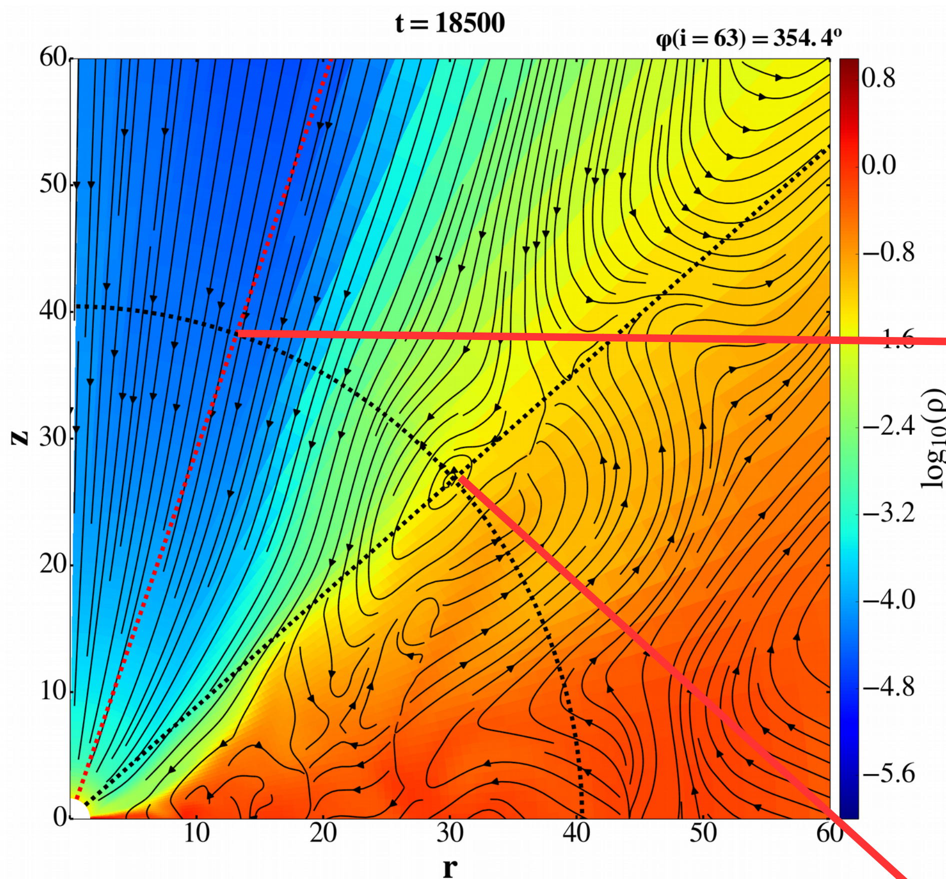

Forces at the same distance from the central object, along a spherical radius line in the corona (red line) and through the magnetic island near the disk surface (black line).

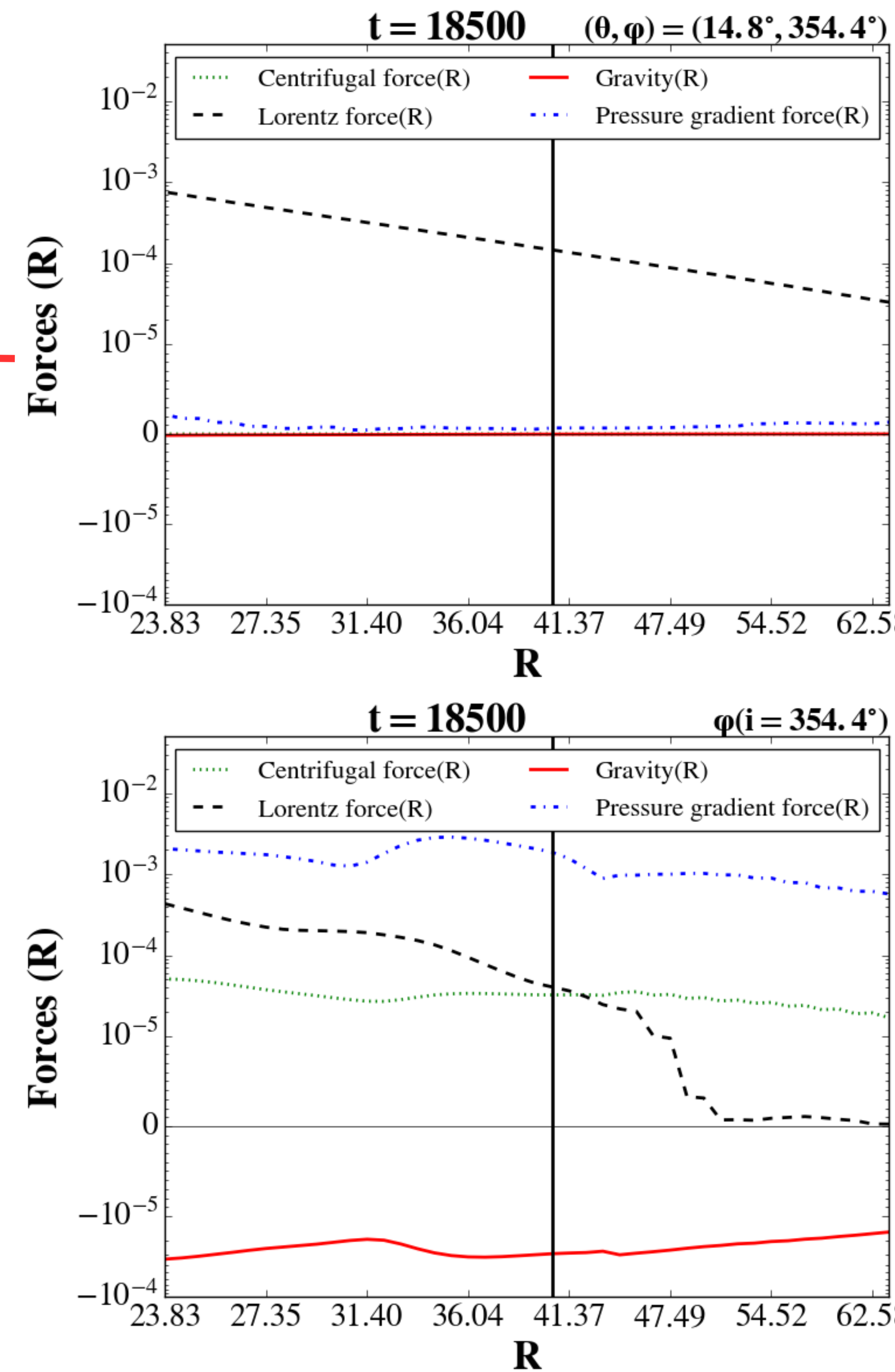

Spiraling-out of the flux ropes

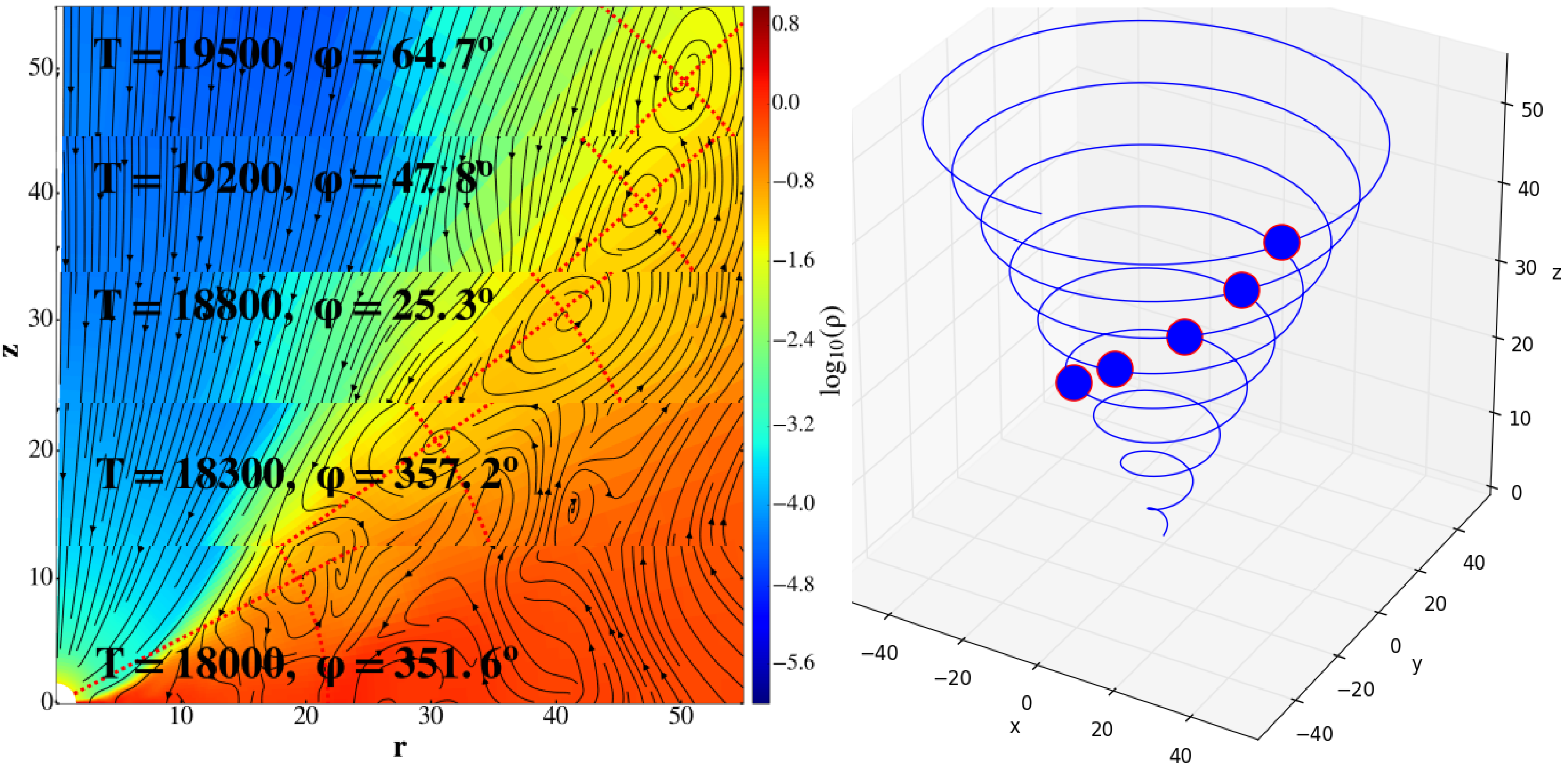

•Slices at different times crossing the middle of the flux rope in our simulation (left panel). The distance from the origin is increasing in time. The angle φ of the colatitudinal plane in which the middle of the flux rope is positioned, is also increasing with time and given in the figure. The flux rope is spiraling away from the black hole, as shown in the 3D schematic plot (right panel) depicting the trajectory of its center.

Ejection of the flux ropes

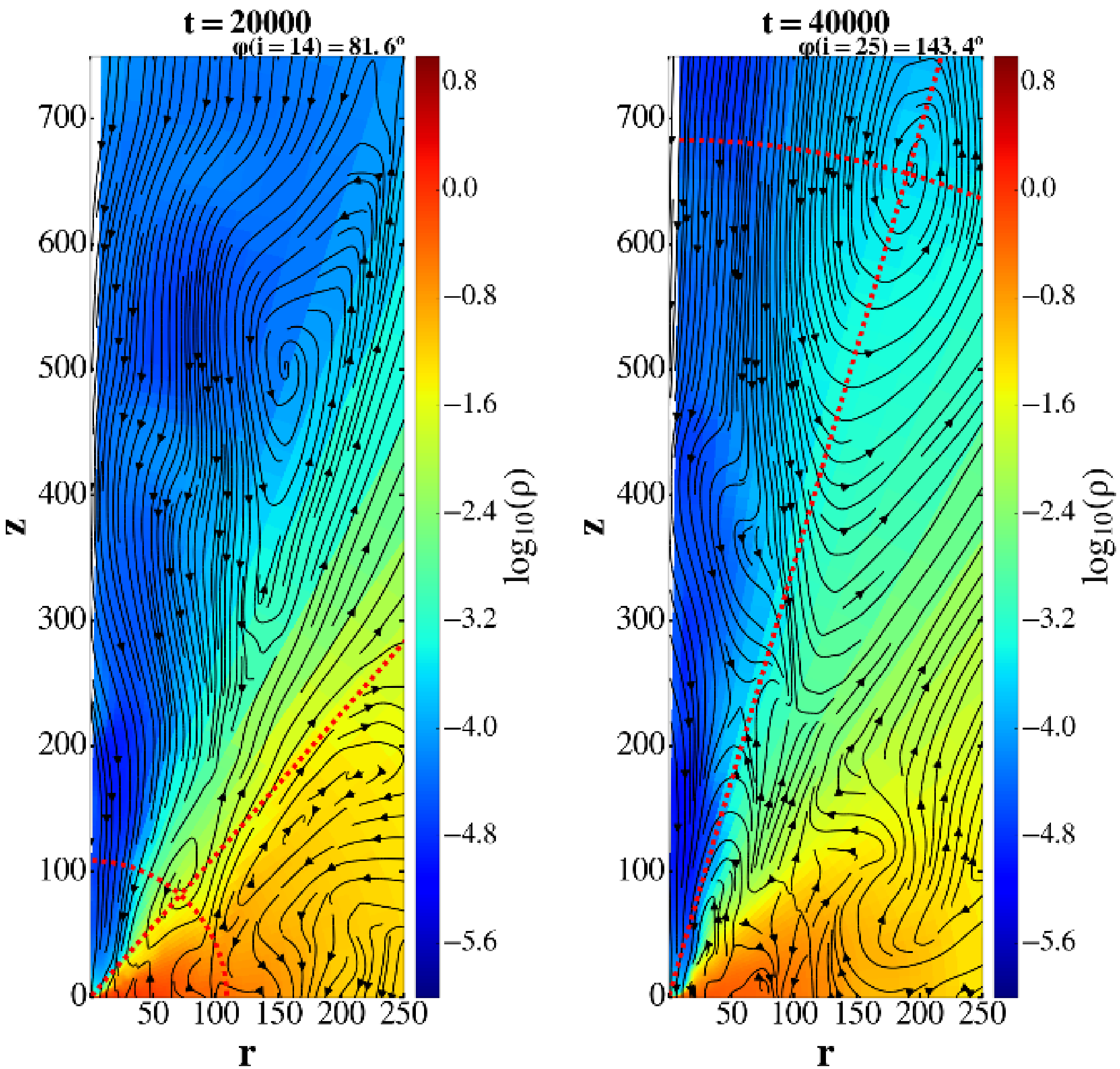

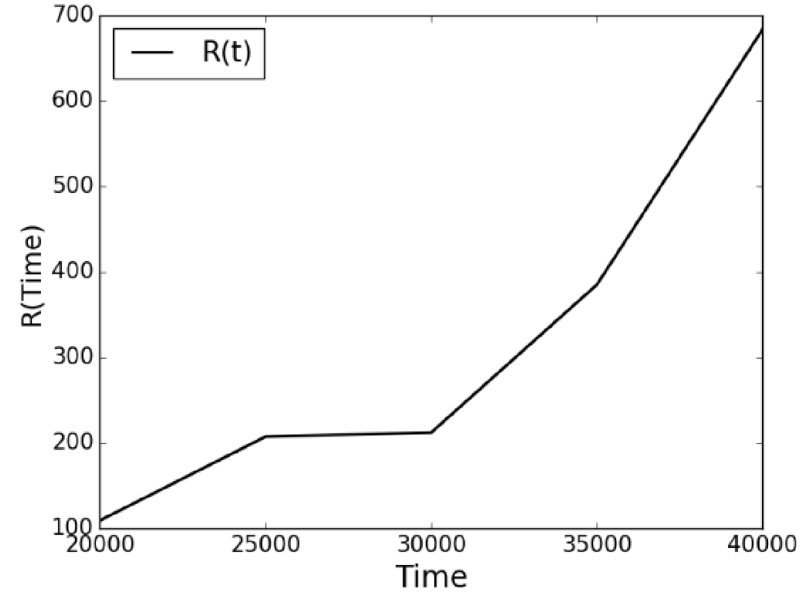

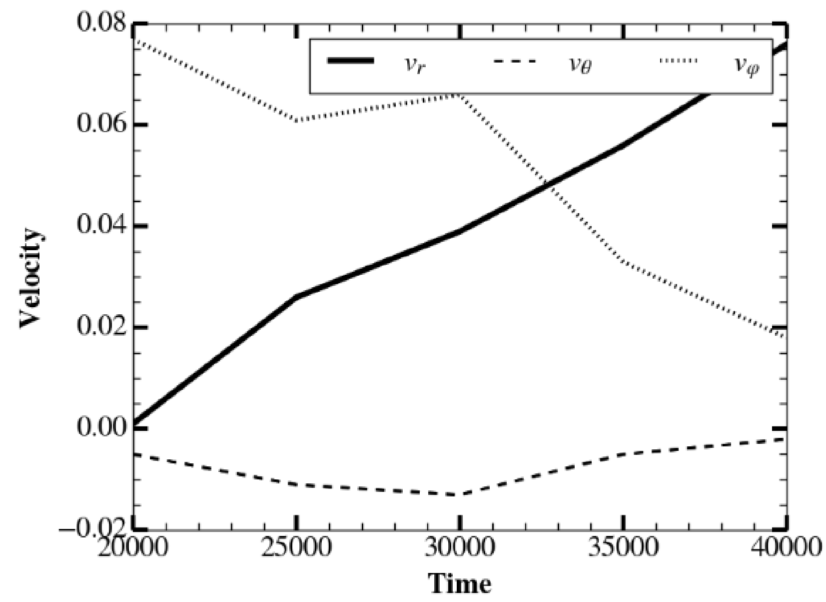

•Slices at different azimuthal planes at times T=20000 and T=40000, during the ejection of the flux rope in the corona. We describe the motion of the flux ropes by following the positions of their centers, and analyze the velocity components along the dashed lines.

Reconnection layers

•A zoom into one of the reconnection layers, with dotted lines along which we compute the physical quantities. Results in both such layers are qualitatively similar, and reconnection layers are connected.

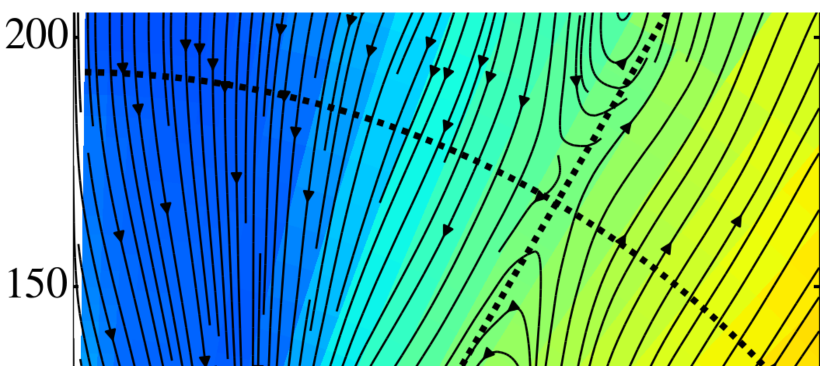

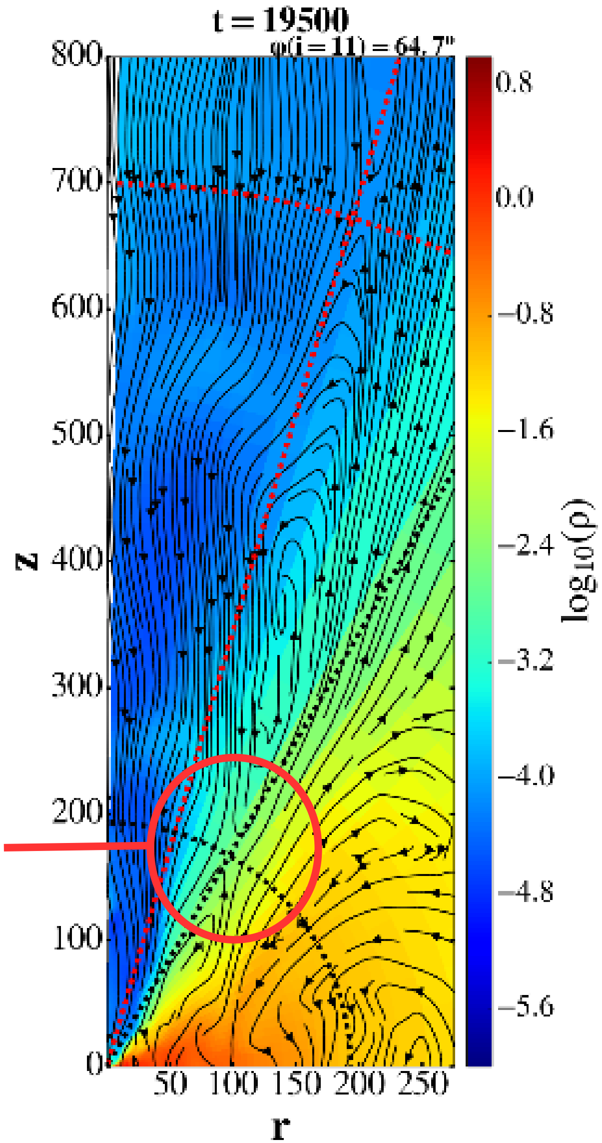

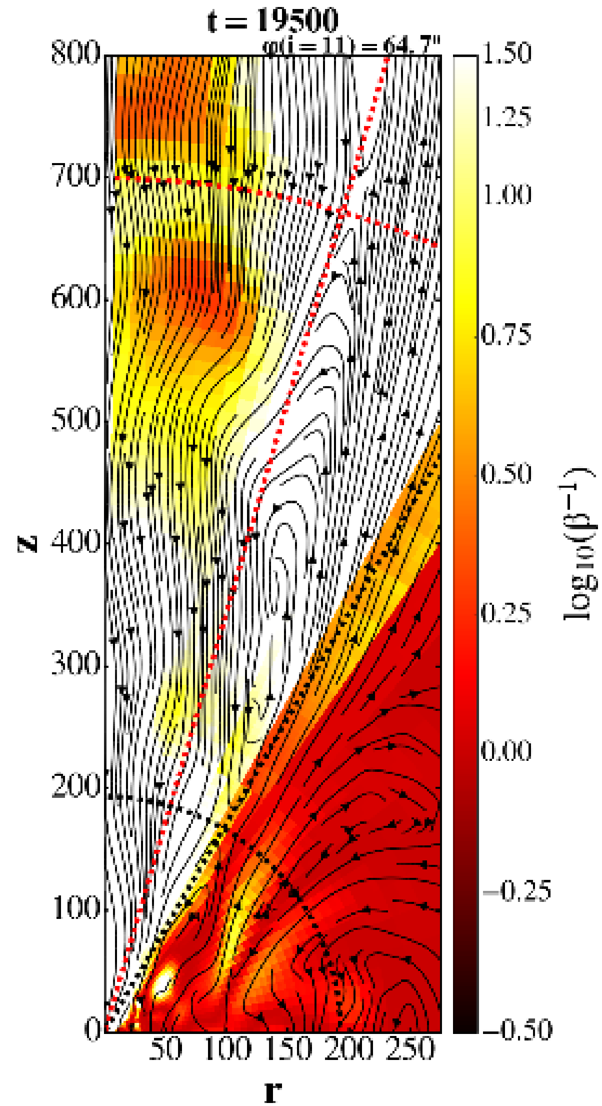

•Reconnection layers in the snapshot at T=19500. In the middle panel are shown the poloidal magnetic field lines with density in logarithmic colour grading as a background, and in the right panel the background is plasma β. With red and black dotted lines are shown the coordinate lines, along which we compute the physical quantities.

Reconnection

Magnetic field (*top panel*) and velocity (*bottom panel*) components as a function of θ across the reconnection layer. Across the reconnection layer all three magnetic field components and two poloidal velocity components change sign.

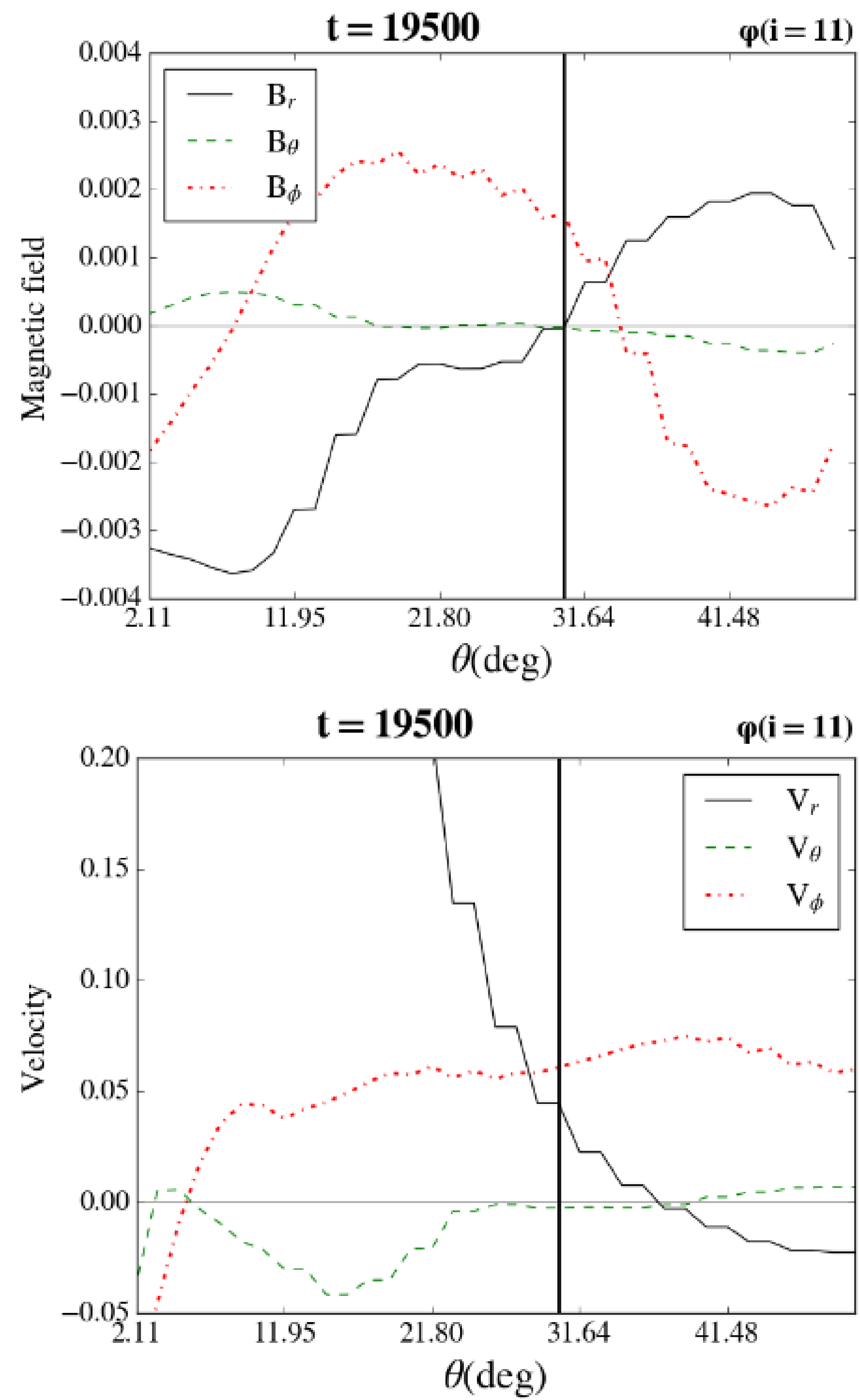

Additional reconection layer

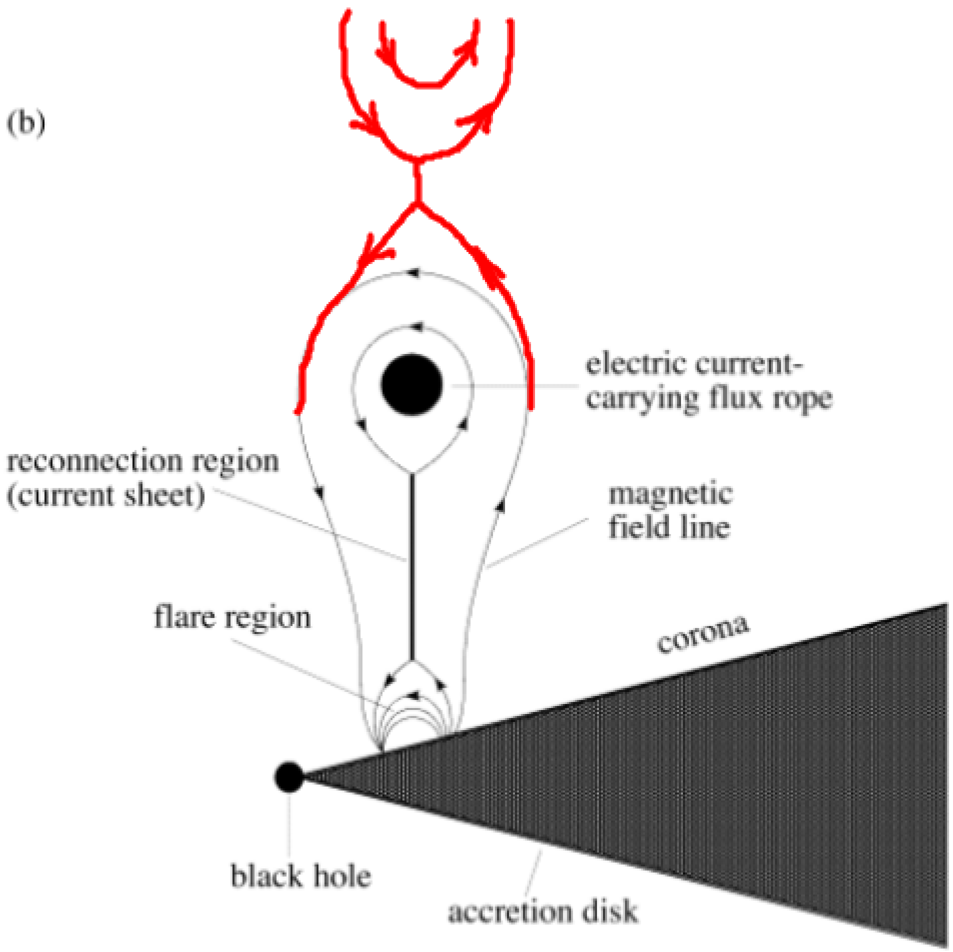

In addition to the reconnection layer below the magnetic flux rope, there is another reconnection layer, above the magnetic flux rope in our simulations. It helps in opening of the magnetic field lines.

Periodicity of the reconnection events and emergence of the magnetic islands

When the magnetic islands are formed in our simulation, their corresponding azimuthal angles φ are usually different, but they emerge periodically from above the disk surface within $20 - 30\ r_g$, every $t = 1000\ r_g/c$. The same time interval we measure between periodic reconnection events at the same position in the computational box.

It is interesting to note that $1000\ r_g/c$ is the Keplerian period at 20-30 r_g.

If scaled to the case of Sgr A*, with the gravitational radius of 6×10^9 m, such an interval gives the period of about 6 hours. It is matching the time-scale of the observed energetic events from this source.

Another periodicity which could have observational consequences would be in the merging of the magnetic islands/flux ropes. In our simulations of the SANE case, such merges seem to happen on at least order of magnitude slower time scale than the emergence of the new magnetic islands.

Summary

- I presented our recent work on formation of magnetic flux ropes in 3D GRMHD numerical simulations with the code Athena++.
- Magnetic structures which show as magnetic islands in 2D simulations, can develop into the magnetic flux ropes in 3D.
- Flux ropes rotate and loop around the central object, similar to the Coronal Mass Ejections (CMEs) on the Sun.
- Because of reconnection, flux ropes are created atop the disk, and are launched into the corona. Additional reconnection layer can form in the corona, further helping the launch.
- Reconnection events which help launching magnetic islands could cause episodic flaring from the vicinity of the disk around a black hole. Scaled to the case of Sgr A*, periodicity of the events would be about 6 hrs.

Thank you!